Positive and negative influences of landfalling typhoons on tropospheric ozone over southern China

Zhixiong Chen[1], Jane Liu[1,2], Xugeng Cheng[1], Mengmiao Yang[1], Hong Wang[3]

[1] Key Laboratory for Humid Subtropical Eco-Geographical Processes of the Ministry of Education, School of Geographical Sciences, Fujian Normal University, Fuzhou, China
[2] Department of Geography and Planning, University of Toronto, Toronto, Ontario, Canada
[3] Fujian Meteorological Administration, Fuzhou, China

Correspondence to: Jane Liu (janejj.liu@utoronto.ca)

Abstract. Based on an ensemble of 17 landfalling typhoons over 2014-2018, we investigate positive and negative influences of typhoons on tropospheric ozone over southern China in this work. Referring to the proximity to typhoon centres and typhoon developmental stages, we find that surface ozone is enhanced when typhoons are 400-1500 km away during the initial stages of typhoons (e.g., from 1 day before and to 1 day after typhoon genesis). The positive ozone anomalies averagely reach 10-20 ppbv above the background ozone level. The maximum enhancement of surface ozone appears at a radial distance of 1100-1300 km from the typhoon centre during these initial stages. As the typhoons approach southern China, the influences of typhoons switch to reducing ozone and hence lead to negative ozone anomalies of 6-9 ppbv. Exploring the linkages between the ozone variations and typhoon-induced meteorological evolutions, we find that during typhoon initial stages, the increasing temperature and weak winds in the atmospheric boundary layer (ABL) and dominating downward motions promote ozone production and accumulation over the outskirts of typhoons. While the deteriorating weather accompanied by dropping temperature, wind gales and convective activity reduces the production and accumulation of surface ozone when typhoons are making landfalling.

We further examine the impacts of landfalling typhoons on tropospheric ozone profiles vertically, especially on the influences of typhoon-induced stratospheric intrusions on lower troposphere and surface ozone. Based on temporally dense ozone profile observations, we find two high-ozone regions separately located in the ABL and the middle-to-upper troposphere during different typhoon stages. Averagely, the one in the ABL is with maximum ozone enhancement of 10-12 ppbv at 1-1.5 km altitude at typhoon initial stages. For the one in the middle-to-upper troposphere, ozone enhancement persists over a longer period with maximum ozone enhancement of ~10 ppbv at 7-8 km altitude shortly after typhoon genesis, and of ~30 ppbv near 12 km altitude when typhoons reach their maximum intensity. When typhoons are landing, negative ozone anomalies appear and extend upward with a maximum ozone reduction of 14-18 ppbv at 5 km altitude and 20-25 ppbv at 11 km altitude. Though the overall tropospheric ozone is usually reduced during typhoon landfalling, we find that five of eight typhoon samples deduce ozone-rich air with the stratospheric origin above 4 km altitude, and in three typhoon cases the

ozone-rich air intrusions can sink to the ABL. This suggests that the typhoon-induced stratospheric intrusions play an important role in surface ozone enhancement.

1 Introduction

It has been noticed that high ozone (O_3) episodes are frequently associated with tropical cyclones (TC) in the warm seasons over southern China (Huang et al., 2005; Lam et al., 2005; Jiang et al., 2008; Shu et al., 2016; Chow et al., 2018; Gao et al., 2020). Previous studies suggested that TCs often modulate meteorological conditions and hence alter photochemical production, accumulation, transport and dispersion of ozone. For example, when TCs approach, the fine and hot weather are associated with strong solar radiation and high temperature, and the overwhelming downward air motions are conducive to low wind speed and stable atmospheric boundary layer (ABL), all of which are responsible for high ozone episodes in the developed and populated Pearl River Delta (PRD) and Yangtze River Delta (YRD) regions (e.g., Shu et al., 2016; Zhan et al., 2020). Still, it is not clear whether these findings of TCs' impacts based on individual cases, are applicable over large domains, e.g., both coastal regions and neighbouring inland provinces in southern China. In recent years, rapid urbanization and economic development also take place in other regions of southern China in addition to PRD and YRD, and many areas suffer from continuous increases in ozone levels (Li et al., 2019; Han et al., 2020). Southern China is frequently under the influences of TCs. There are around 326 TCs formed over the western Pacific during 2000-2017 (Li et al. 2020), and averagely six typhoons make landfall annually in southern China (Zhang et al., 2013). Therefore, it is urgently needed to statistically investigate the influences of TC on tropospheric ozone over southern China, given the frequent TC activities from June to October and the close connections between TC and high ozone episodes.

Typhoons, also named hurricanes in the Atlantic and the eastern North Pacific, refer to the intensive kind of TCs with maximum sustained wind speeds exceeding 37.2 m s^{-1}. The typhoons that finally make their landfall in China raise more concerns due to their relatively larger sizes, higher severities, and more direct passages toward coastal regions and neighbouring inland provinces in southern China. Though TCs have been regarded as one of the main synoptic patterns influencing surface ozone concentrations, a comprehensive understanding of ozone variations in space and time attributable to landfalling typhoons is lacking, as previous studies generally were limited to individual cases or regional domains, and were mostly focused on ozone enhancement only. A typhoon circulation typifies a radius of $O(10^3$ km) and can persist for several days with varied intensities and locations that steer ozone behaviour differently. From the occurrences of ozone episodes and the spatiotemporal distribution and property of typhoons, Huang et al. (2006) found that when a typhoon is about 700-1000 km away from the PRD, the region is already controlled by large-scale subsidence of typhoon and suffers high ozone pollution. Roux et al. (2020) stated that typhoons at a distance of 500-1000 km offshore provide a favourable environment for active photochemical reactions and hence high ozone episodes. It is also documented that surface ozone concentrations increase over southwestern Taiwan 2 to 4 days before the passage of typhoons (Hung and Lo, 2015). Recently, Zhan et al. (2020) found that in YRD ozone pollution episodes mainly occur when a typhoon reaches the 24-h warning line (thick dashed line in Fig. 1) and the previous typhoon dies away in mainland China. While it is of value to stress typhoon-induced ozone enhancement in the context of air pollution, the cleansing function associated with landfalling typhoons is also important for a complete evaluation of typhoon influences on surface ozone concentrations and on long-term

tropospheric ozone trends. Hence, a full insight into the evolutionary influences of landfalling typhoons, i.e., both ozone enhancement and reduction effects, would further our understanding of the contribution of typhoons to surface ozone variations and tropospheric ozone.

Typhoons consist of bands of convective clouds that can vertically penetrate into the tropopause region. Therefore, they can potentially perturb the structure and chemical compositions in the tropopause region, and promote stratosphere-troposphere exchanges (STEs). For example, several studies show that typhoons can induce the downward intrusions of ozone-rich air (Jiang et al., 2015; Das et al., 2016; Li et al., 2018; Roux et al., 2020). Such intrusions can even reach the ABL and deteriorate air quality there, as in the case of Typhoon Hagibis over southeastern coast of China reported by Jiang et al. (2015). However, some previous studies emphasized the role of typhoons in cleaning the air and reducing tropospheric ozone concentrations. They hold that the stratospheric intrusions of ozone-rich air are insignificant, and instead, the uplifting of marine ozone-poor airmass by typhoons decreases tropospheric ozone concentrations. In a recent study, Li et al. (2020) analysed 18-year ozonesonde measurements at a frequency of once per week over Hong Kong and Naha, and found that TC including typhoons reduce ozone by ~20–60 ppbv from the mean near the tropopause. Noticing the positive and negative influences of typhoons on tropospheric ozone, researchers pointed out that such different influences are closely related to development stages and intensities of typhoons (e.g., Zou and Wu 2005; Midya et al., 2012). Therefore, given the evolving features of typhoons, sufficient ozone observations are necessary to adequately sample the fine-scale structure of ozone and hence quantitatively address the influence of typhoon-induced stratosphere intrusion to tropospheric ozone. Unfortunately, few studies have been done because a large ensemble of typhoons and temporally dense ozone vertical observations are required to provide statistically robust results.

In this study, we comprehensively investigate the successive response of ozone concentrations to landfalling typhoons over southern China. A large ensemble of landfalling typhoon cases over 2014-2018 is applied to examine the overall ozone behaviours and hence offers statistically reliable conclusions. The landfalling typhoons are divided into several developmental stages to track their evolutionary features of location and intensity. Accordingly, the multiple impacts of typhoons on surface ozone variations, namely, the positive (enhancement) and negative (reduction) impacts during the entire lifespan of typhoons are analysed and gauged. Given the importance of stratospheric intrusions to tropospheric ozone budget, the evolution of ozone profiles during landfall typhoons is analysed to quantify the contribution of external descending stratospheric ozone to lower tropospheric ozone. To realize this, temporally dense observations, including ground-based ozone and vertical ozone profiles collected during typhoon seasons, are synchronized according to typhoon developmental features. Meteorological conditions are also analysed to reveal the physical linkages between typhoon evolutions and ozone variations in time and space. We intend to answer the following scientific questions:

(1) How do surface ozone concentrations vary spatiotemporally under the influences of landfalling typhoons? What are meteorological factors responsible for such ozone variations?

(2) How the tropospheric ozone profiles respond to the differential developmental stages of landfalling typhoons? What are meteorological controls on the vertical ozone variations?

(3) Do the typhoon-induced stratospheric intrusions play a significant role in enhancing troposphere and surface ozone?

The remaining paper is structured as follows. Section 2 describes the study domain and period, the ozone observations, meteorological data, and analysis methods. Section 3 presents the statistical distributions of surface ozone concentrations with reference to typhoon developmental features. Section 4 shows the vertical variations of ozone concentrations during the evolutionary processes of landfalling typhoons based on temporally dense ozone profile observations. The impacts of typhoon-induced STE on the vertical ozone distributions is also presented. Section 5 offers the conclusions, discussions, and suggestions for future work.

2 Data and method

2.1 Typhoon data

The best track data of tropical cyclones for China is provided by the China Meteorological Center (CMA) (available at: http://tcdata.typhoon.org.cn/ zjljsjj_sm.html, last access: 25 Oct 2021) (Ying et al., 2014). The TCs can be classified into several categories according to their averaged wind speed, namely, tropical depression (TD, with wind speed of 10.8-17.1 m s^{-1}), tropical storm (TS, with wind speed of 17.2-24.4 m s^{-1}), severe tropical storm (STS, with wind speed of 24.5-32.6 m s^{-1}), typhoon (TY, with wind speed of 32.7- 41.4 m s^{-1}), severe typhoon (with wind speed of 41.5-50.9 m s^{-1}) and super typhoon (Super TY, with wind speed exceeding 51.0 m s^{-1}). We extracted the information about each typhoon over 2014-2018, including storm category, geolocation of cyclone centers (latitude and longitude), minimum sea level pressure, and maximum sustained wind speed. The information of best tracks is collected every 6 hours from 1949, and since 2017 it is updated to every 3 hours to better capture the typhoon evolution during its landfall.

The landfalling typhoons attract much attention due to their severity and direct passages toward densely populated lands. A total of 17 typhoons landed in China over 2014-2018 as shown in Fig. 1, which form a large ensemble for investigating impacts of typhoons on the overall ozone behaviours with high confidence. Given the evolving nature of typhoons with varied location and intensity, we divide typhoon development into several stages with reference to the timing of their genesis, first-time maximum intensity and landfalling. The genesis time (hereafter T_g) is obtained from the best track data when the typhoon is first identified in TD category. Pre-typhoon periods are examined before 1 day (T_g-1d) and 2 days (T_g-2d) of T_g, and the conditions right after +1 day (T_g+1d) are also included in our study. The time of maximum intensity of typhoons (T_{max}) is determined when the maximum sustained wind speed peaks (also lowest minimum sea level pressure) for the first time. The time of landfalling ($T_{landing}$) is determined when typhoons first land in southern China and $T_{landing}$+1d represent the post-landfalling conditions +1 day after the typhoon landfall. Therefore, there are 7 developmental stages in total to represent evolutionary characteristics of the entire typhoon lifespan. By sequence, they are T_g-2d, T_g-1d, T_g, T_g+1d, T_{max}, $T_{landing}$ and $T_{landing}$+1d. Ozone and meteorological conditions in the typhoon ensemble are synchronized according to the divided 7 stages and compared to illustrate how ozone varies with distance to typhoons at the different typhoon developmental stages in southern China.
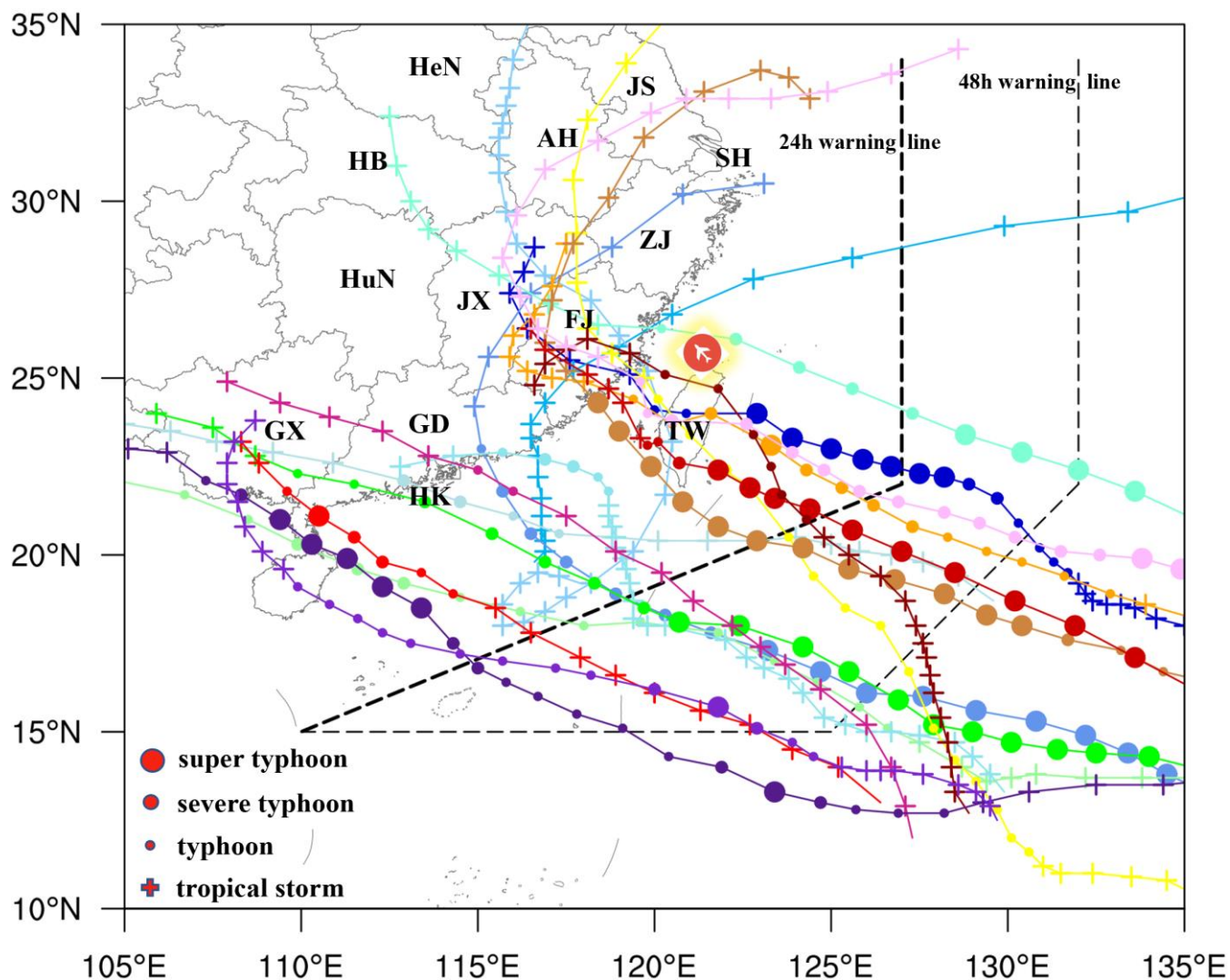
Figure 1: The tracks (lines) and categories (symbols) of 17 landfalling typhoons over the western Pacific over 2014-2018. The thin and thick black dashed lines represent the 48-h and 24-h typhoon warning lines, respectively. The locations and boundaries for the provinces of interest are indicated by the corresponding abbreviations for Anhui (AH), Fujian (FJ), Guangdong (GD), Guangxi (GX), Henan (HeN), Hubei (HB), Hunan (HuN), Jiangsu (JS), Jiangxi (JX), and Zhejiang (ZJ). Shanghai (SH) district is also showed. The location, where vertical ozone profiles are available at Taoyuan International Airport (25.076 °N, 121.224 °E) of Taiwan (TW), is marked with a red plane symbol.

2.2 Ground-based ozone observations

Routine measurements of surface air pollutants are provided by the China National Environmental Monitoring Centre. This nationwide network consists of more than 1500 stations distributed over 454 cities. Each station hourly measures six

types of air pollutants including surface fine particles with an aerodynamic diameter of 2.5 μm (PM2.5) and of 10 μm (PM$_{10}$),

145   ozone (O$_3$), carbon monoxide (CO), nitrogen dioxide (NO$_2$) and sulfur dioxide (SO$_2$) (Lu et al., 2018). The observational data are strictly quality controlled and can be accessed via a real-time air quality reporting website (http://106.37.208.233:20035/, last access: 25 Oct 2021).

This study focuses on the evolutionary impacts posed by typhoons on ozone concentrations over the coastal regions and neighbouring inland areas in southern China (Fig. 1). The hourly surface ozone concentrations in each city are calculated by

150   averaging the observations from all the monitoring stations in that city. Two specific hours, the 1400 local standard time (LST, = 0600 UTC) and the 0200 LST (= 1800 UTC), are in coincidence with typhoon observation timing and used to represent typical ozone scenarios during the daytime and nighttime, respectively.

Provided with the geolocation of cities and typhoon centers, the radial distances between the ozone observation and the corresponding typhoon centers are calculated at each of the typhoon developmental stage for all the cities. Then these ozone

155   concentrations are spatially averaged with a spacing of 200 km in radial direction. A background value of surface ozone concentrations (T$_{avg}$) is also calculated as the baseline by averaging the corresponding observations during the typhoon seasons (from June to October) over 2014-2018. Note in this calculation, the geolocation of typhoons at T$_g$ stage is used. For ozone features in pre-typhoon conditions at T$_g$-2d and T$_g$-1d, the geolocation of typhoon at stage T$_g$ is also applied as the typhoons are not generated yet. Ozone variations along the radial direction of each typhoon and at typhoon developmental

160   stages are repeatedly calculated and averaged for taking mean ozone concentrations over the typhoon ensemble.

2.3 Airborne-based ozone observations

Airborne measurements of atmospheric chemical compounds are provided by the European Research Infrastructure program IAGOS (In-service Aircraft for a Global Observing System, https://www.iagos.org, last access: 25 Oct 2021) (Petzold et al., 2015). O$_3$, CO, nitrogen oxides (NO$_x$) as well as temperature, winds and relative humidity are measured by

165   the in-situ sensors during flights around the world. For O$_3$, it is measured by a dual-beam UV absorption monitor operated at 253.7 nm, and the concentrations are automatically corrected for pressure and temperature influences. The response time of O$_3$ measurement is 4 s, and the accuracy of ozone observations is estimated to be at ±2 ppbv (Thouret et al., 1998).

Sufficient IAGOS observations are collected during take-offs and landings at Taoyuan International Airport (25.076 °N, 121.224 °E, red plane symbol in Fig. 1) in Taiwan (TW). Considering data quality, the airborne observations associated with

170   landfalling typhoons over 2014-2018 are screened and eight typhoons are selected. The ozone profiles are analysed with reference to the seven developmental stages of typhoons defined above. In the end, we obtain 234 profiles in total with 21 profiles for the genesis stage of typhoons and 34 for maximum stage and 29 for landfalling stage. These temporally dense ozone profiles guarantee to adequately resolve the successive response of ozone distribution to different typhoon stages, and hence provide a comprehensive insight into contributions of typhoons to tropospheric ozone budget. The ozone profile data

175   are processed into a uniform 100-m vertical resolution by averaging observations over 100 m thick layers from 0 to 12 km above sea level. Same as the processing of surface ozone observations, the ozone profiles associated with each

developmental stages of each typhoon are averaged over the typhoon ensemble. The vertical profiles of temperature and wind observations are processed in the same way.

2.4 Reanalysis meteorological data

180   The typhoon-induced meteorological influences on ozone are analysed using the MERRA-2 (The Modern-Era Retrospective Analysis for Research and Applications, Version 2) reanalysis data, which are produced by NASA's Global Modeling and Assimilation Office (GMAO, https://gmao.gsfc.nasa.gov/ reanalysis/MERRA-2, last access: 25 Oct 2021). The MERRA-2 data have a spatial resolution of 0.5 $^\circ\times$ 0.625 $^\circ$ and 72 vertical levels. The reanalysis data have been evaluated and found to match well with the observations from Chinese weather stations (Li et al., 2019). The gridded
185   meteorological variables, including temperature, wind, vertical velocity and potential vorticity (PV), are extracted from MERRA-2 during each of the typhoon developmental stages to investigate meteorological linkages to the production, accumulation, transport, dispersion of ozone.

3 Surface ozone concentrations affected by landfalling typhoons

Fig.1 shows the tracks and categories of the 17 landfalling typhoons during the period of 2014–2018. These typhoons
190   are marked with 4 categories ranging from tropical storm to typhoons, severe typhoons and super typhoons. Among the 17 landfalling typhoon cases, 11 of them was developed into the super typhoon intensity. Typhoons landed on Taiwan (TW), Fujian (FJ) and Guangdong (GD) provinces most frequently, and kept travelling to influence neighbouring inland regions. Given a typical size of typhoon circulations at an order of 1000 km, these landfalling typhoons have the potential to influence large-scale meteorological environments and hence impact surface ozone concentrations over southern China.
195   Previous studies show that surface ozone concentrations in PRD and YRD are enhanced when typhoons are 700-1000 km away and when typhoons cross the 24-h warning line (thick black dashed line in Fig. 1) (e.g., Huang et al., 2006; Zhan et al., 2020). Extending from these findings of ozone enhancement over the distant regions from typhoon centres, this paper examines overall variations in surface ozone with the radial distance of landfalling typhoons over southern China, and comprehensively addresses both positive and negative impacts of typhoons on surface ozone as follows.
200   Fig.2 shows surface ozone concentrations varying along the radial distance of typhoons at different typhoon developmental stages, based on the mean of the 17 landfalling typhoon samples. During the daytime (1400 LST, Fig. 2a), the background ozone concentrations range between 45-55 ppbv with small variations along the radial direction of typhoons. Surface ozone concentrations are obviously elevated from the pre-typhoon conditions (T_g-2d and T_g-1d) to the typhoon genesis (T_g and T_g+1d). The averaged ozone enhancement reaches 10-20 ppbv when typhoons are 400-1500 km away, which
205   produces positive anomalies of 20-40% from T_g-2d to T_g+1d above the background ozone concentrations. Particularly, surface ozone concentrations are largest within radial distances of 1100-1300 km with a mean magnitude of 83.4 ppbv during T_g-1d and T_g stages, yielding positive anomalies of 52.5% against the background ozone concentrations of 54.7 ppbv.

During the nighttime (0200 LST, Fig. 2b) when the ozone photochemical reactions cease, positive ozone anomalies of ~9 ppbv relative to the background ozone concentrations persist during T_g-1d and T_g stages. The zone with significant ozone enhancement is generally similar to that during the daytime. Considering the necessity of ozone episode warning, based on the consistent behaviours of ozone enhancement at daytime and nighttime behind a large ensemble of landfalling typhoons, we suggest that surface ozone concentrations at a radial distance of 1100-1300 km are most significantly enhanced during the initial stages of typhoons.
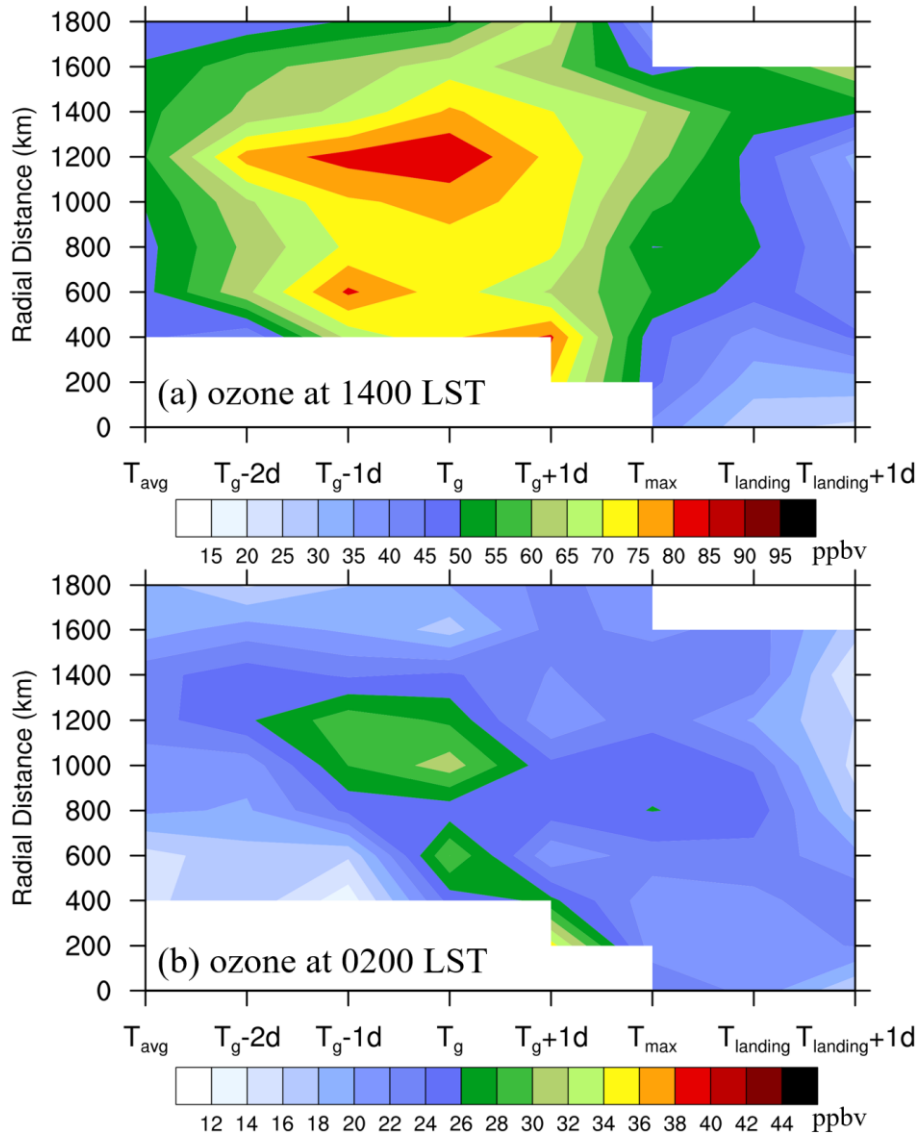
Figure 2: Surface ozone concentrations (unit: ppbv) varying along the radial distance of typhoons at various typhoon developmental stages at daytime (a) and nighttime (b). The concentrations are the mean ozone concentrations of all the typhoons

220   As the typhoons develop rapidly and approach southern China westward, the typhoon influences on surface ozone switch from enhancement to reduction. An obvious region with low ozone concentrations appears right after the T_{max} stage when the typhoons have reached their maximum intensity and move closer to the coast. Surface ozone concentrations fall into its background levels at T_{max} stage and keep decreasing when the typhoons make landfall in southern China. Quantitatively, the negative ozone anomalies are -11.9 % (6 ppbv) at $T_{landing}$ and -16.6 % (9 ppbv) at $T_{landing}$ +1d stage

225 relative to the background ozone concentrations at daytime. Between T_{max} and $T_{landing}$ +1d stage, surface ozone concentrations decrease monotonously with the decrease in the radial distance to the typhoon centres. In other words, partly due to the arrival of marine airmass, ozone is greatly reduced near the typhoon centers.

     To understand large changes in typhoon's influences on surface ozone from enhancing to cleansing ozone during the lifespan of typhoons, we explore meteorological connections between the evolutionary typhoons and successive response of

230 surface ozone from perspectives of ozone production, accumulation, transport, and dispersion. Similar to the analysis applied to surface ozone, meteorological variables are processed with consideration of the radial distance and developmental stages of the landfalling typhoons. Fig. 3 shows the evolutions of air temperature and wind speed within ABL, and 500-hPa vertical air motions averaged over the 17 typhoons using the MERRA-2 reanalysis. From T_g-2d to T_g+1d stages, a systematic increase of air temperature is noticed both in near-surface 10-m and 850-hPa height within a radial distance of 400-1500 km

235 to the typhoon centers at daytime (Fig. 3a). Taking the air temperature as a proxy of solar radiation intensity, it can be inferred that the boundary layer is dominated by fine and hot weather accompanied with strong solar radiation that promotes the photochemical production of ozone during these stages. In terms of wind fields, belt-like regions with weak winds (< 3-4 m s^{-1}) are found when typhoons are 800-1600 km away from T_g-2d to T_g+1d stages (Fig. 3b). The low wind speed zone extends up from surface to 850 hPa, yielding a stable ABL that is favourable for accumulation of ozone. Regarding vertical

240 flows, downward air motions dominate in the mid troposphere over the outskirts of typhoons (800-1500 km in radial direction). This peripheral subsidence of typhoons contributes to the cloudless conditions and a stable structure of ABL, which are favourable to ozone production and accumulation. The meteorological scenario at nighttime is similar to that at daytime that support the persistency of promoted ozone contents except that the ozone photochemical reaction ceases due to lack of sunshine. During the early initial stages of typhoons, stagnation with low wind speed under the control of the

245 typhoons is also significant and accompanied by the systematic downward motions between 800-1200 km in radial direction at night (0200 LST) as shown in Fig. 4.
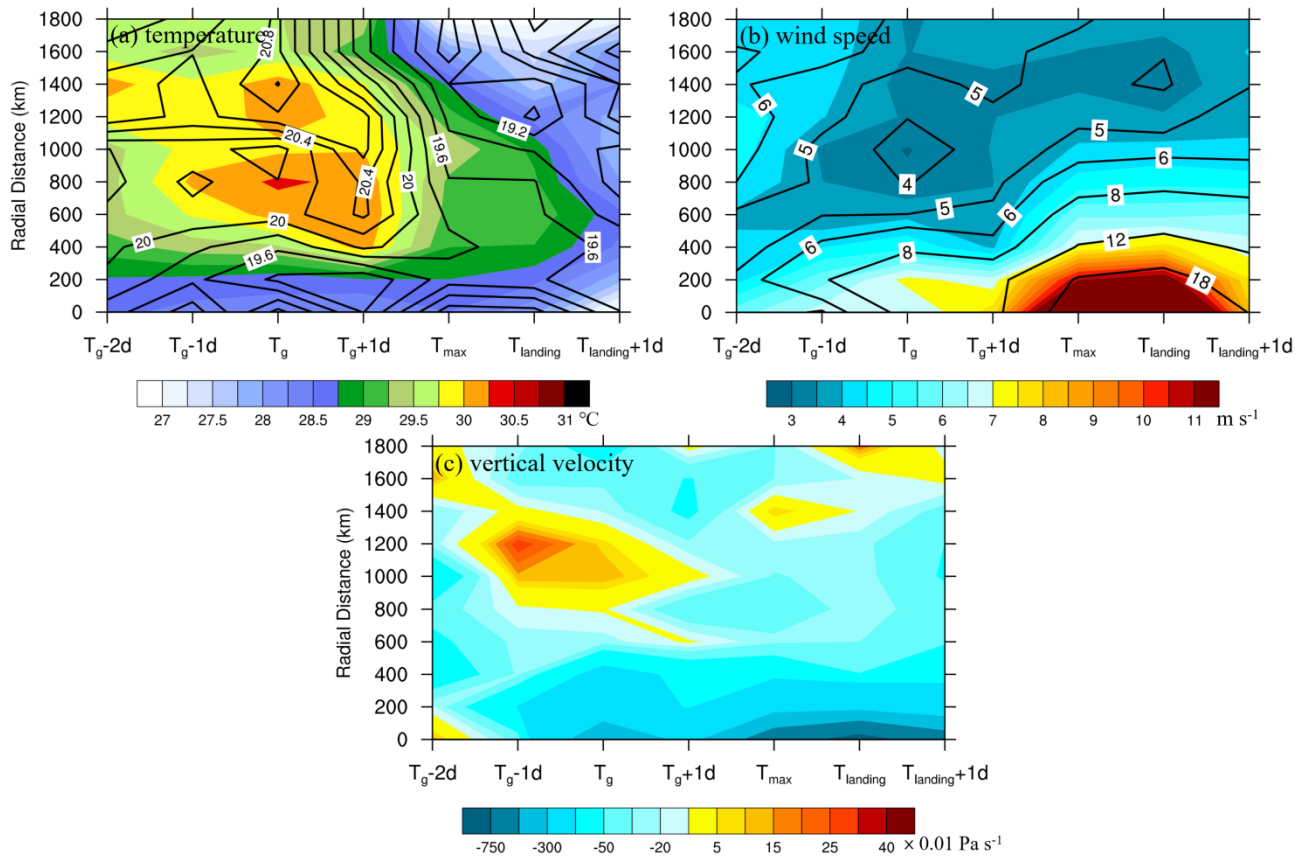
Figure 3: (a) 10-m (shaded) and 850-hPa (contour lines) air temperature (unit: °C), (b) 10-m (shaded) and 850-hPa (contour lines) wind speed (unit: m s⁻¹) and (c) 500-hPa vertical wind velocity (unit: 0.01 Pa s⁻¹, positive values for downward air motions and vice versa) at daytime (1400 LST) based on MERRA-2 reanalysis at different radial distances and typhoon developmental stages averaged over the large ensemble of typhoons over 2014-2018.

Along with the westward advance of the typhoons, the weather begins to deteriorate and surface ozone concentrations drop after T_g+1d stage. The cloudy environments and convective activities take over the previous fine and hot weather. The air temperature drops significantly and the wind speed increases steadily from T_{max} to $T_{landing}$ +1d stages that reduce accumulation of surface ozone (Fig. 3 and Fig. 4). As the typhoons approaching southern China, gales (wind speed > 10 m s⁻¹) appear and bring in ozone-poor marine airmass. The upward vertical motions intensify over land and give rise to cloud formation and precipitation, which further reduce ozone concentrations.
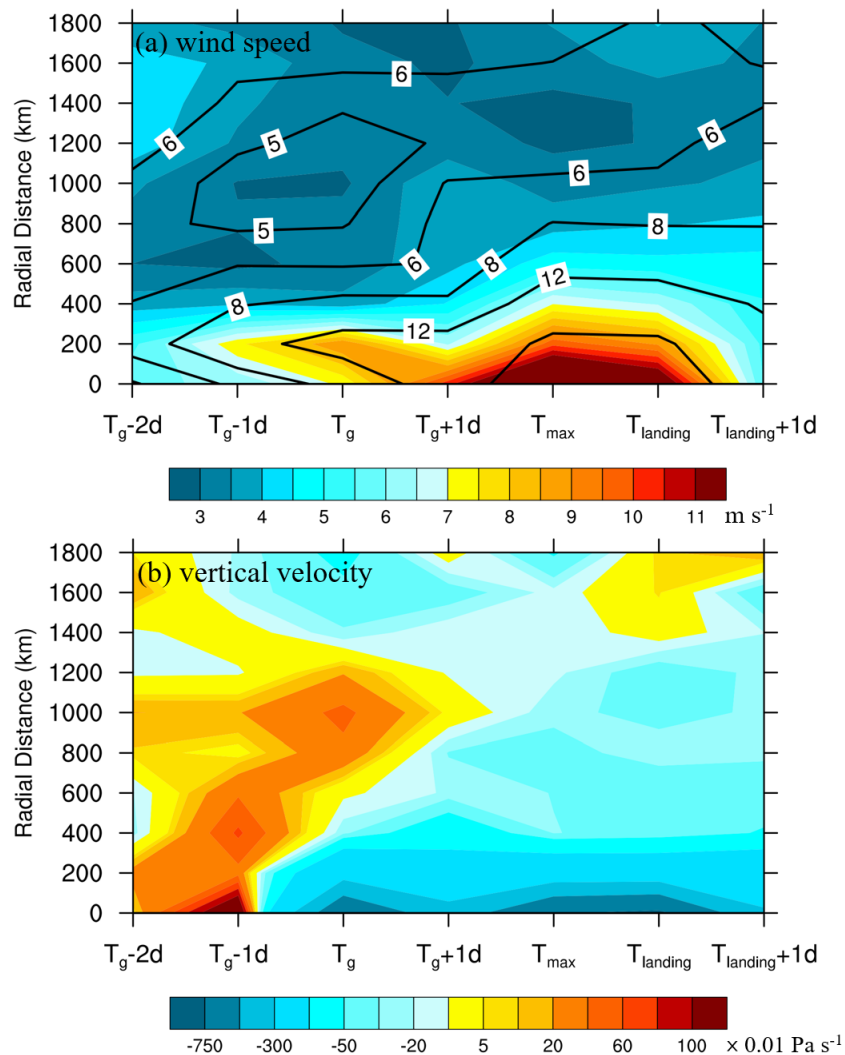
260 **Figure 4: Same as Fig. 3b-c, but for nighttime (0200 LST).**

The above analysis presents the physical linkages between landfalling typhoons, meteorological conditions and surface ozone variations. The overall meteorological conditions associated with different typhoon developmental stages alter production, accumulation, transport, and dispersion of ozone and lead to different influences from enhancing to cleansing ozone pollution along with typhoon development. Practically, these results of the spatiotemporal variations of ozone when a typhoon is approaching raise challenging demands for observation and numerical forecasting of typhoon development. The necessary information about the timing and location of typhoon genesis as well as pre-typhoon conditions, are only available from reliable numerical forecasting. Therefore, to capture the evolutionary ozone behaviours over southern China during typhoon landfalling, not only chemical aspects of models are required to describe the reactions between atmospheric compositions, but also meteorological conditions in models should be improved to forecast the developmental stages of

270 typhoons. Note that the analysis in this section is mainly related to the typhoon influences on ozone production and loss within the ABL. Several studies suggest that typhoon-induced STEs can bring ozone-rich airmass from the lower stratosphere and thus enhance surface ozone. Therefore, the variations of vertical ozone profiles are analysed for assessing the typhoon influences on tropospheric ozone using temporally dense vertical observations in the next section.

4 Vertical ozone distributions affected by landfalling typhoons

275 It is reported that typhoons may enhance or reduce tropospheric or surface ozone concentrations (e.g., Jiang et al., 2015; Das et al., 2016; Li et al., 2020), which is probably related to the developmental stages and intensity changes of typhoons. Therefore, dense vertical ozone observations are required given the rapid evolutions in intensity and location of typhoons. Using airborne observations of atmospheric compositions under the IAGOS framework, Roux et al. (2020) analysed the ozone profiles collected at Taoyuan International Airport (25.076 °N, 121.224 °E) of Taiwan (TW, Fig. 1) during the 2016
280 typhoon season. They found elevated ozone in the middle and upper troposphere and tracked back to its stratospheric origin. In this study, the ozone vertical profiles measured during taking-off and landing of flights at Taoyuan airport with dense temporal resolutions are collected and processed according to the developmental stages of the typhoon ensemble. A total of 234 ozone profiles covering each divided stage of typhoons guarantee that the evolutionary variation in ozone profiles in response to typhoon developments can be well captured.

285 The averaged vertical ozone profiles at each typhoon developmental stage are shown in Fig. 5a. At T_g-2d stage, ozone concentrations range between 30-45 ppbv below 4 km altitude and increase slightly to 45-60 ppbv in the middle-to-upper troposphere. Starting from T_g-1d stage, ozone concentrations in all layers increase with different magnitudes. Vertically, there appear two separated regions with high ozone abundances, one in the middle ABL and the other in the middle-to-upper troposphere. The high ozone abundances in the troposphere mainly have two sources (Zhan et al., 2020), e.g., active ozone
290 photochemical reactions at daytime in the boundary layer and downward intrusions of ozone-rich air from upper levels. The dense airborne observations show that ozone enhancement below 2 km altitude is only significant in the pre-typhoon and initial stages (T_g-1d and T_g), suggesting the dependence of photochemical reactions on meteorological conditions controlled by typhoons. Simultaneous measurements of temperature and winds via the flights (Fig. 6a and 6b) show that a peak positive temperature anomaly of 0.3 °C is located at 1.5 km altitude during T_g-1d and T_g compared against that of T_g-2d stage, which
295 is accompanied by a weak wind zone (< 6 m s^{-1}) promoting ozone production and accumulation in the boundary layer. Though the warming continues in the low troposphere due to the approaching warm core of typhoons, wind flows intensify rapidly in the ABL and exceed 10 m s^{-1} that effectively transports clean air mass and lead to lower ozone concentrations after T_g+1d stage. In the middle-to-upper troposphere, ozone is enhanced and thus a region of high ozone concentrations of 75-80 ppbv appears at an altitude of 12 km at T_{max} stage. As shown in Fig. 6c, the overall vertical air flows shift from weak
300 subsidence to intensifying upward motions that perturbate the structure of tropopause. The decreasing tropopause might facilitate the stratosphere-to-troposphere exchange and provide chances for ozone-rich air in the lower stratosphere to intrude

to the troposphere. This may explain an asynchronous evolution of ozone in the boundary layer and middle-to-upper troposphere.
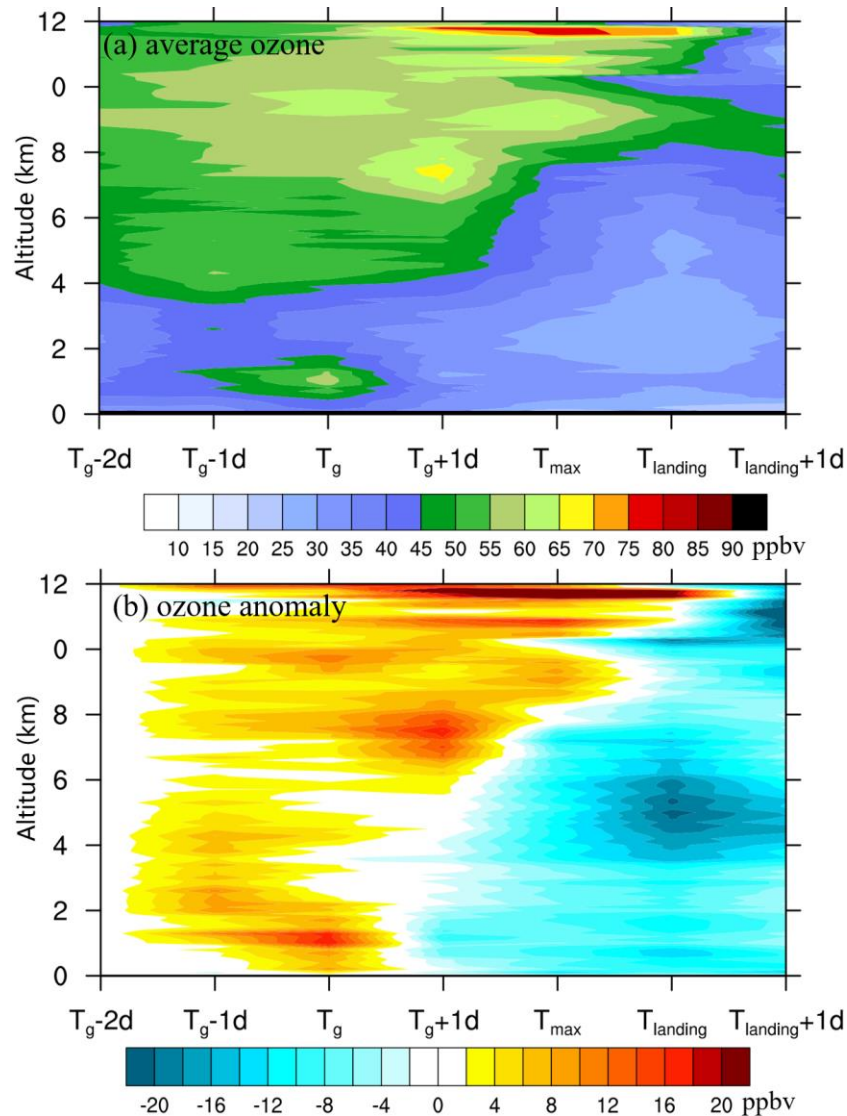
305 **Figure 5: (a) Vertical ozone concentrations (unit: ppbv) at each typhoon developmental stage averaged over the typhoon ensemble over 2014-2018 at Taiwan. (b) Anomalies of vertical ozone concentrations relative to Tg-2d stage of the subsequent typhoon developmental stages. The temporally dense ozone profiles are available from the airborne observations of atmospheric compositions under the IAGOS framework collected at Taoyuan International Airport of Taiwan.**

Taking ozone concentrations at T_g-2d as the references, a tilted structure of ozone anomalies is obvious (Fig. 5b) due to 310 the asynchronous evolution in different heights. Quantitatively, the maximum magnitude of ozone variations is 10-12 ppbv at 1-1.5 km altitude, equalling to a 25 % positive ozone anomaly at T_g stage in the boundary layer. The results are consistent

with Zhan et al. (2020) who suggested that ozone is mainly generated inside the boundary layer (~ 1 km) instead of at the surface. In the middle-to-upper troposphere, positive ozone anomalies persist over long time within a deep layer (4-12 km). The positive ozone anomalies reach 10 ppbv at 7-8 km altitude at T_g+1d stage and 30 ppbv near 12 km altitude at T_{max} stage. However, along with typhoon development, negative ozone anomalies form and stretch upward from T_g+1d stage, which probably is a compromise between upward transport of clean marine airmass and downward transport of ozone-rich air from upper levels. Hence, there appear largest negative differences of 14-18 ppbv around 5 km altitude at $T_{landing}$ stage and of 20-25 ppbv around 11 km altitude at $T_{landing}$+1d stage relative to ozone concentrations at T_g-2d stage.
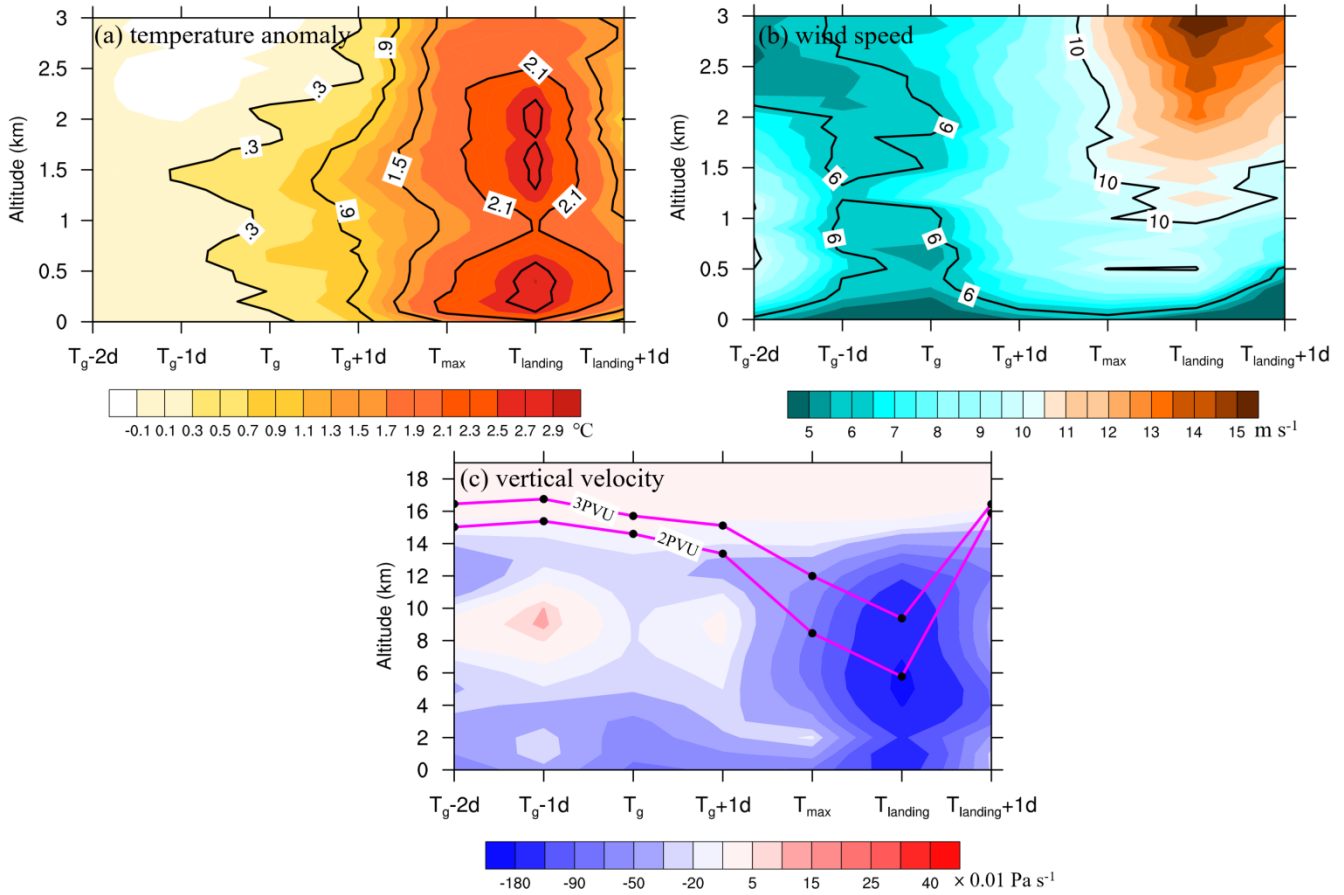
Figure 6: (a) Temperature anomalies relative to T_g-2d (unit: °C) and (b) wind speed at each typhoon developmental stage within the boundary layer using the simultaneous flight observations at Taoyuan International Airport of Taiwan. (c) Vertical velocity (shaded, unit: 0.01 Pa s^{-1}) and the average height of 2-PVU (potential vorticity units, 1 PVU = 10−6 m2 s−1 K kg−1) and 3-PVU regions. The data are averaged over the large ensemble of typhoons over 2014-2018.

The above analysis is based on the observational mean of eight typhoons over 2014-2018, suggesting that tropospheric ozone concentrations are reduced by clean marine airmass caused by the strong uplift in landfalling typhoons. Another question is how frequently the ozone-rich airmass from the upper levels can sink down to the lower troposphere and even

enhance surface ozone during the passing of typhoons. Reported in case studies by Das et al. (2016), the typhoon-induced downward propagation of airmass can bring high ozone from the upper to the lower troposphere. Considering that such downward transport of ozone-rich air mass could be easily smoothed by averaging all samples (e.g., Fig 5), we reexamine

330 these temporally dense ozone observations by counting the number of ozone concentrations (every 10 ppbv) in each vertical layer (with a 100-m spacing) at different developmental stages of typhoons (Fig. 7). As mentioned above, a combination of high temperature and weak winds in the boundary layer promotes the active ozone photochemical production and accumulation at T_g-1d and T_g stages. Large ozone concentrations up to 130–160 ppbv below 2 km altitude are observed (black arrows in Fig. 7b-c). After T_g+1d stage, high ozone episodes in the boundary layer cease due to deteriorated weather,

335 however, the number of high ozone concentrations grows in the upper troposphere. Using 80 ppbv as a threshold for ozone with stratospheric origin, based on the averaged ozone concentrations in Fig. 5a, we find that the intrusions of stratospheric ozone-rich air largely appear above 4 km altitude (red arrows in Fig. 7d-f). Despite some mixing processes with ambient air, the stratospheric air mass can also sink down to the lower boundary layer (below 2 km altitude). As shown in the black circles in Fig. 7d-f, the number of ozone concentrations over 60 ppbv rises at T_{max} stage compared with those at T_g+1d and

340 $T_{landing}$ stages, which evidently confirms the contribution of external stratospheric ozone to lower troposphere ozone. With a quantitative overview of the vertical ozone variations in the eight typhoons, we find that five of them deduce stratospheric intrusions and, in three of them, the ozone-rich stratospheric airmass sink down to the ABL. Though ozone concentrations are reduced in the entire tropospheric column vertically when typhoons are making landfalling, surface ozone can be enhanced by the downward propagation of stratospheric ozone-rich air.
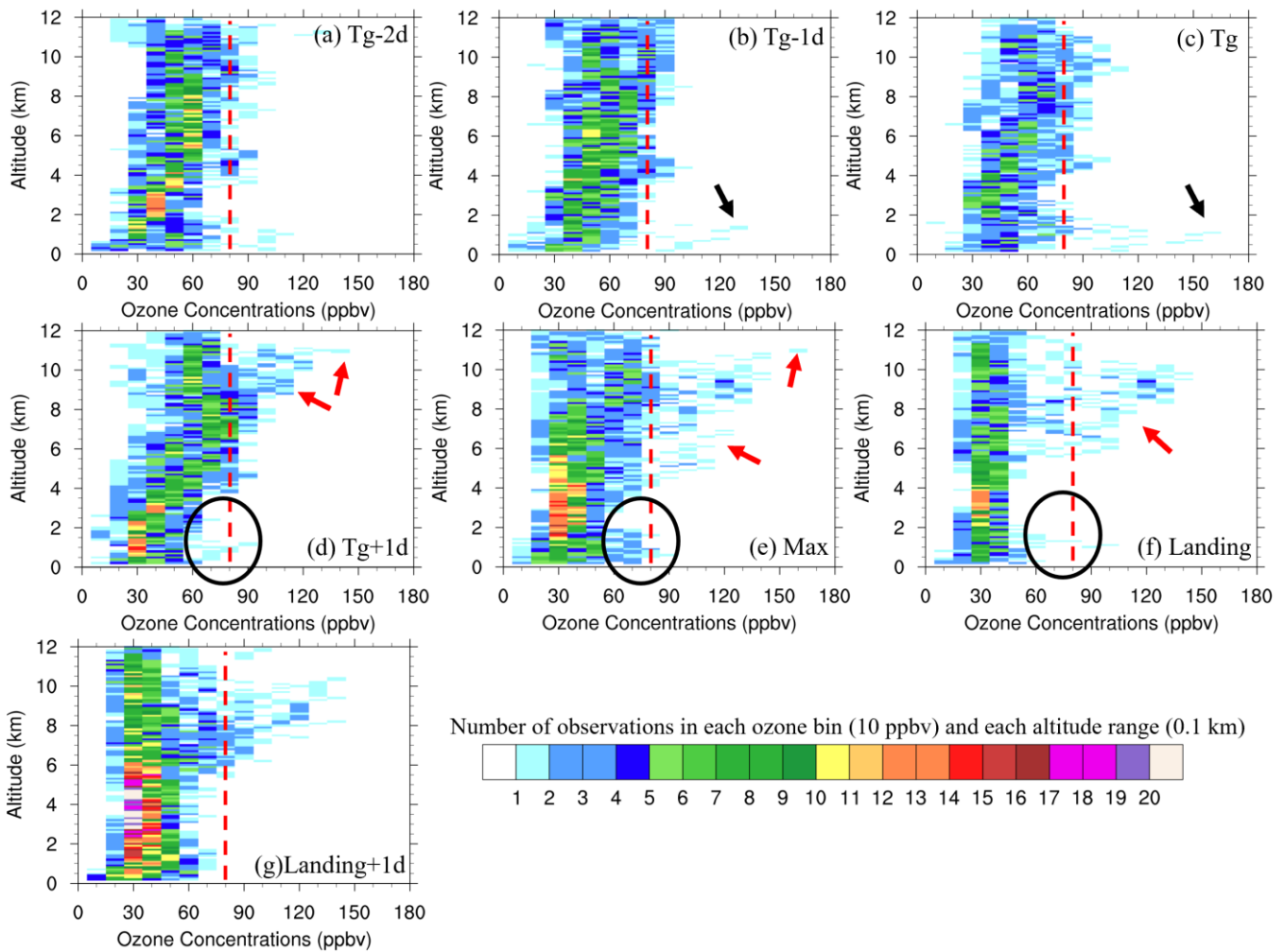
345

Figure 7: Number of ozone concentrations (every 10 ppbv) in each vertical layer (with a 100-m spacing) at different developmental stages of typhoons. The red dashed lines of 80 ppbv represent ozone-rich air mass with stratosphere origin based on the averaged results in Fig. 5a.

5 Conclusions, discussions and suggestions

350   In previous studies, influences of typhoons on ozone in the atmospheric boundary layer were investigated over the developed and populated regions in China, such as PRD and YRD. Given the severity of ozone pollution during rapid urbanization and economic development in southern China, it is of importance to address and quantify impacts of typhoons on ozone over larger domains that are frequently under controls of typhoons. In this study, we use an ensemble of 17 landfalling typhoons over 2014-2018 (Fig. 1) to investigate the positive and negative influences of typhoons on tropospheric

355   ozone over southern China. Both the proximity to typhoons and typhoon developmental stage are taken into account to

reveal the evolutionary response of tropospheric ozone to landfalling typhoons. We find that surface ozone is enhanced when typhoons are 400-1500 km away during the initial stages of typhoons (e.g., from 1 day before and to 1 day after typhoon genesis). On average, the positive ozone anomalies reach 10-20 ppbv at the daytime (1400 LST) and 9 ppbv at nighttime above the background ozone level. Surface ozone concentrations at radial distances of 1100-1300 km are most significantly enhanced during the initial stages of typhoons. As the typhoons move closer to southern China westward, the influences of typhoons change from enhancing to reducing ozone. Then, typhoons reach their maximum intensity and keep decreasing in their intensity when they make landfall, and surface ozone concentrations are reduced with negative ozone anomalies of -12 % ~ -17 % (6~9 ppbv) relative to the background ozone level. The linkages between typhoons, meteorological conditions, and ozone are investigated. A combination of high air temperature, weak winds in the ABL and dominating downward motions promotes the photochemical production and accumulation of ozone over the outskirts of typhoons during their initial stages. When typhoons are making landfalling, the deteriorating weather accompanied by dropping temperature and wind gales reduces the production and accumulation of surface ozone. Ozone-poor marine airmass are brought to inland. In addition, the intensified upward vertical motions give rise to cloud formation and precipitation and further hinder ozone formation and accumulation.

Besides the processes in the ABL influenced by typhoons, we also investigate variations in tropospheric ozone profiles during the differential developmental stages of landfalling typhoons. In particular, we examine how the typhoon-induced stratospheric intrusions alter lower troposphere and surface ozone. Based on the temporally dense ozone vertical observations collected at Taiwan during eight typhoons, we find two regions with cores of high ozone abundances separately located in the ABL and the middle-to-upper troposphere. In the ABL at the initial stages of typhoons, ozone below 2 km altitude is generally enhanced because of the warming air and low wind speed. Then ozone concentrations decrease continuously when wind intensifies rapidly that transport the clean air mass. In the middle-to-upper troposphere, ozone enhancement persists over a long period and generates a region with high ozone concentrations (75-80 ppbv at 12 km altitude). The tropopause is perturbated with decreasing tropopause height as typhoons develop, which might provide chances of stratospheric intrusions that bring downward ozone-rich air from the lower stratosphere. The asynchronous evolutions of ozone in the ABL and middle-to-upper troposphere lead to a tilted structure of ozone anomalies vertically along typhoon evolutions (Fig. 5). Averagely, positive ozone anomalies maximize around 10-12 ppbv at 1-1.5 km altitude at the initial stages of typhoons. In the middle-to-upper troposphere, the positive ozone anomaly is 10 ppbv at 7-8 km altitude shortly after typhoon genesis, and 30 ppbv near 12 km altitude when typhoons reach their maximum intensity. When typhoons are landing, negative ozone anomalies stretch upward with a maximum ozone reduction of 14-18 ppbv at 5 km altitude and 20-25 ppbv at 11 km altitude relative to the pre-typhoon conditions.

We further assess the impacts of typhoon-induced disturbances in the upper troposphere that bring ozone-rich air downward at different developmental stages of typhoons (Fig. 7). During the initial typhoon stages, high ozone (130–160 ppbv) below 2 km altitude are observed, which can be attributed to active ozone photochemical production and accumulation processes. After typhoon genesis, ozone-rich air from the stratosphere is more frequently observed above 4 km altitude, and

even propagates downward to the lower boundary layer (below 2 km altitude) despite some mixing processes with ambient air. We find that in the eight typhoons with ozone profile observations covering the entire typhoon lifespan, five of them deduce ozone-rich air with the stratospheric origin, and in 3 typhoon cases the intrusions can penetrate down to the ABL. This suggests that surface ozone is possibly enhanced by the downward propagation of stratospheric ozone-rich air when typhoons reach their maximum intensity, though the tropospheric column ozone is usually reduced after landings of typhoons.

Using a large ensemble of typhoons and temporally dense ozone observations, this study characterizes spatiotemporal variations in tropospheric ozone under the influence of typhoons over southern China, a region with frequent typhoon activities. We investigate positive and negative influences of typhoons on surface ozone and tropospheric ozone vertically. The impact of typhoon-induced stratospheric intrusions is quantitatively examined to find possibility of surface ozone episodes resulting from upper-level ozone sources. Still, further studies are needed to better assess the contributions of different chemical and physical processes to ozone concentrations in the ABL and to assess the role of STEs in increasing tropospheric and surface ozone during typhoons. Intensive observations of vertical ozone profiles are highly demanded over different typhoon regimes, and hence ozonesonde measurements at Fujian province is initiated to complement airborne ozone observations at Taiwan, both of which are frequent landing spots of typhoons. Numerical simulations of meteorological and chemical evolutions during typhoons, for example, using the Weather Research and Forecasting (WRF) model coupled with Chemistry (WRF-Chem), provide a way to analyse ozone variations at fine scale. However, both the meteorological and chemical simulations need to be improved so the evolutionary features of ozone during typhoon landfalling can be captured. Also, previous studies stressed the lightning associated with intensive convection of typhoons can produce nitrogen oxides (LNO_x) and hence influence ozone chemical reactions (Kaynak et al., 2008; Roux et al., 2020; Das et al., 2016). In addition to lightning occurrences and LNO_x, the deep convection of typhoons can also transport ozone by dynamically dragging down the stratospheric ozone-rich air. Pan et al. (2014) reported that the ozone-rich stratospheric air wraps around both leading and trailing edges of a mesoscale convective system and descends to lower levels. Hence a better representation of the LNO_x influence on chemical reactions and meteorology concerning dynamical transport should be included in the typhoon simulations. Currently, we are incorporating data assimilation (DA) to improve WRF-Chem simulations. We are developing a three-dimensional variational DA scheme to assimilate lightning observations over the data-sparse oceans to update meteorological conditions (Chen et al., 2020) and LNO_x presentations (Allen et al., 2010; Pickering et al., 2016; Kang et al., 2019).

Data Availability Statement

The track data of tropical cyclones for China used in the present study can be obtained from http://tcdata.typhoon.org.cn/ zjljsjj_sm.html. The surface air pollutant observations obtained from the China National Environmental Monitoring Centre can be obtained from http://106.37.208.233:20035/. The airborne measurements of

atmospheric chemical compounds provided by the European Research Infrastructure program IAGOS can be downloaded from https://www.iagos.org. The MERRA-2 reanalysis meteorological data can be downloaded from https://gmao.gsfc.nasa.gov/reanalysis/MERRA-2.

425

Author contributions

ZC and JL designed the study and performed the research. ZC collected the observations and analyzed the data. ZC and JL wrote and revised the paper, with input from XC, MY, and HW. All authors commented on drafts of the paper.

Competing interests

430   The authors declare that they have no conflict of interest.

Acknowledgments

This work was supported by the National Natural Science Foundation of China (Grants 42105079). The computing resources used in this study were provided by Fujian Normal University High Performance Computation Center (FNU-HPCC). We also acknowledge the free use of flight-based atmospheric chemical measurements from IAGOS. IAGOS is 435   funded by the European Union projects IAGOS-DS and IAGOS-ERI. The IAGOS database is created with support from the European Commission, national agencies in Germany (BMBF), France (MESR), and the UK (NERC), and the IAGOS member institutions (http://www.iagos.org/partners). The participating airlines (Lufthansa, Air France, Austrian, China Airlines, Iberia, Cathay Pacific, Air Namibia, Sabena) supported IAGOS by carrying the measurement equipment free of charge since 1994. We thank the constructive comments and suggestions from the anonymous reviewers.

440   **References**

Allen, D., Pickering, K., Duncan, B., and Damon, M.: Impact of lightning NO emissions on North American photochemistry as determined using the Global Modeling Initiative (GMI) model, J. Geophys. Res., 115, D22301, https://doi.org/10.1029/2010JD014062, 2010.

Chen, Z., Sun, J., Qie, X., Zhang, Y., Ying, Z., Xiao, X., and Cao, D.: A method to update model kinematic states by 445   assimilating satellite-observed total lightning data to improve convective analysis and forecasting. J. Geophys. Res., 125, JD033330, https://doi.org/10.1029/2020JD033330, 2020.

Chow, E. C., Li, R. C., and Zhou, W.: Influence of tropical cyclones on Hong Kong air quality, Adv. Atmos. Sci., 35(9), https://doi.org/10.1007/s00376-018-7225-4, 2018.

Das, S. S., Ratnam, M. K., Uma, K. N., Subrahmanyam, K. V., Girach, I. A., Patra, A. K., Aneesh, S., Suneeth, K. V., Kumar, K. K., Kesarkar, A. P., Sijikumar, S., and Ramkumar, G.: Influence of tropical cyclones on tropospheric ozone: Possible implications, Atmos. Chem. Phys., 16, 4837–4847, https://doi.org/10.5194/acp-16-4837-2016, 2016.

Gao, D., Xie, M., Chen, X., Wang, T., Liu, J., Xu, Q., Mu, X., Chen, F., Li, S., Zhuang, B., Li, M., Zhao, M., and Ren, Y.: Systematic classification of circulation patterns and integrated analysis of their effects on different ozone pollution levels in the Yangtze River Delta Region, China, Atmos. Environ., 242 ,117760, https://doi.org/10.1016/j.atmosenv.2020.117760, 2020.

Han, H., Liu, J., Shu, L., Wang, T., and Yuan, H.,: Local and synoptic meteorological influences on daily variability in summertime surface ozone in eastern China, Atmos. Chem. Phys., 20, 203–222, https://doi.org/10.5194/acp-20-203-2020, 2020.

Huang, J. P., Fung, J. C. H., Lau, A. K. H., and Qin, Y.: Numerical simulation and process analysis of typhoon-related ozone episodes in Hong Kong, J. Geophys. Res., 110, D05301, https://doi.org/10.1029/2004JD004914, 2005.

Huang, J. P., Fung, C. H., and Lau, K. H.: Integrated processes analysis and systematic meteorological classification of ozone episodes in Hong Kong, J. Geophys. Res., 111, D20309, https://doi.org/10.1029/2005JD007012, 2006.

Hung, C.-H. and Lo, K.-C.: Relationship between ambient ozone concentration changes in southwestern Taiwan and invasion tracks of tropical typhoons, Adv. Meteorol., 2015, 402976, https://doi.org/10.1155/2015/402976, 2015.

Jiang, F., Wang, T., Wang, T., Xie, M., and Zhao, H.: Numerical modeling of a continuous photochemical pollution episodein Hong Kong using WRF–chem, Atmos. Environ., 42(38), 8717–8727, https://doi.org/10.1016/j.atmosenv.2008.08.034, 2008.

Jiang, Y., Zhao, T., Liu, J., Xu, X., Tan, C., Cheng, X., Bi, X., Gan, J., You, J., and Zhao, S.: Why does surface ozone peak before a typhoon landing in southeast China, Atmos. Chem. Phys., 15, 13331-13338, https://doi.org/10.5194/acp-15-13331-2015, 2015.

Kang, D., Pickering, K., Allen, D., Foley, K., Wong, D., Mathur, R., and Roselle, S.: Simulating lightning NO production in CMAQv5.2: evolution of scientific updates, Geosci. Model. Dev., 12(7), 3071-3083, https://doi.org/10.5194/gmd-12-3071-2019, 2019.

Kaynak B., Hu Y., Martin RV, Russell AG, Choi Y, and Wang Y: The effect of lightning NOx production on surface ozone in the continental United States, Atmos. Chem. Phys, 8, 5151–5159, https://doi.org/10.5194/acp-8-5151-2008, 2008.

Lam, K. S., Wang, T. J., Wu, C. L., and Li, Y. S.: Study on an ozone episode in hot season in Hong Kong and transboundary air pollution over Pearl River Delta region of China, Atmos. Environ., 39(11), 1967-1977, https://doi.org/10.1016/j.atmosenv.2004.11.023, 2005.

Li, D., Vogel, B., Müller, R., Bian, J., Günther, G., Li, Q., Zhang, J., Bai, Z., Vömel, H., and Riese, M.: High tropospheric ozone in Lhasa within the Asian summer monsoon anticyclone in 2013: influence of convective transport and stratospheric intrusions, Atmos. Chem. Phys., 18, 17979-17994, https://doi.org/10.5194/acp-18-17979-2018, 2018.

Li, D., Baerbel, V., Rolf, M., Bian, J., Günther, G., and Riese, M.: Tropical cyclones reduce ozone in the tropopause region

over the western Pacific: An analysis of 18 years ozonesonde profiles, Earth's Future, 9, e2020EF001635, https://doi.org/10.1029/2020EF001635, 2020.

485 Li, K., Jacob, D. J., Liao, H., Shen, L., Zhang, Q., and Bates, K. H.: Anthropogenic drivers of 2013–2017 trends in summer surface ozone in China, P. Natl. Acad. Sci. USA, 116(2), 422-427, https://doi.org/10.1073/pnas.1812168116, 2019.

Lu, X., Hong, J., Zhang, L., Cooper, O. R., Schultz, M. G., Xu, X., Wang, T., Gao, M., Zhao, Y., and Zhang, Y.: Severe Surface Ozone Pollution in China: A Global Perspective, Environ. Sci. Technol. Lett., 5, 487-494, https://doi.org/10.1021/acs.estlett.8b00366, 2018.

490 Midya, S. K., Dey, S. S., and Chakraborty, B.: Variation of the total ozone column during tropical cyclones over the Bay of Bengal and the Arabian Sea, Meteorol. Atmos. Phys., 117, 63-71, https://doi.org/10.1007/S00703-011-0169-1, 2012.

Pan, L. L., Homeyer, C. R., Honomochi, S., Ridley, B. A., Weisman, M., Barth, M. C., Hair, J. W., Fenn, M. A., Butler, C., Diskin, G. S., Crawford, J. H., Ryerson, T. B., Pollack, I., Peischl, J., and Huntrieser, H.: Thunderstorms enhance tropospheric ozone by wrapping and shedding stratospheric air, Geophys. Res. Lett., 41, 7785-7790,
495 https://doi.org/10.1002/2014GL061921, 2014.

Petzold, A., Thouret, V., Gerbig, C., Zahn, A., Brenninkmeijer, C. A. M., Gallagher, M., Hermann, M., Pontaud, M., Ziereis, H., Boulanger, D., Marshall, J., Nédélec, P., Smit, H. G. J., Friess, U., Flaud, J.-M., Wahner, A., Cammas, J.-P., Volz-Thomas, A., and IAGOS TEAM: Global-scale atmosphere monitoring by in-service aircraft – current achievements and future prospects of the European Research Infrastructure IAGOS, Tellus B, 67, 1-24,
500 http://dx.doi.org/10.3402/tellusb.v67.28452, 2015.

Pickering, K. E., Bucsela, E., Allen, D., Ring, A., Holzworth, R., and Krotkov, N.: Estimates of lightning NOx production basedon OMI NO2 observations over the Gulf of Mexico, J. Geophys. Res., 121, 8668-8691, https://doi.org/10.1002/2015JD024179, 2016.

Roux, F., Clark, H., Wang, K.-Y., Rohs, S., Sauvage, B., and Nédélec, P.: The influence of typhoons on atmospheric
505 composition deduced from IAGOS measurements over Taipei, Atmos. Chem. Phys., 20, 3945-3963, https://doi.org/10.5194/acp-20-3945-2020, 2020.

Shu, L., Xie, M., Wang, T., Gao, D., Chen, P., Han, Y., Li, S., Zhuang, B., and Li, M.: Integrated studies of a regional ozone pollution synthetically affected by subtropical high and typhoon system in the Yangtze River Delta region, China, Atmos. Chem. Phys., 16, 15801-15819, https://doi.org/10.5194/acp-16-15801-2016, 2016.

510 Thouret, V., Marenco, A., Logan, J. A., Nédélec, P., and Grouhel, C.: Comparisons of ozone measurements from the MOZAIC airborne program and the ozone sounding network at eight locations, J. Geophys. Res., 103, 25695-25720, https://doi.org/10.1029/98JD02243, 1998.

Ying, M., Zhang, W., Yu, H., Lu, X., Feng, J., Fan, Y., Zhu, Y., and Chen, D.: An overview of the China Meteorological Administration Tropical Cyclone Database, J. Atmos. Ocean. Technol., 31, 287-301, https://doi.org/10.1175/JTECH-D-
515 12-00119.1, 2014.

Zhan, C., Xie, M., Huang, C., Liu, J., Wang, T., Xu, M., Ma, C., Yu, J., Jiao, Y., Li, M., Li, S., Zhuang, B., Zhao, M., and Nie,

D.: Ozone affected by a succession of four landfall typhoons in the Yangtze River Delta, China: major processes and health impacts, Atmos. Chem. Phys., 20 (22), 13781-13799, https://doi.org/10.5194/acp-20-13781-2020, 2020.

Zhang, W., Leung, Y., and Chan, J. L. C.: The analysis of tropical cyclone tracks in the western North Pacific through data mining, Part I: Tropical Cyclone Recurvature, J. Appl. Meteor. Climatol., 52, 1394-1416, https://doi.org/10.1175/JAMC-D-12-045.1, 2013.

Zou, X. and Wu, Y.: On the relationship between Total Ozone Mapping Spectrometer (TOMS) ozone and hurricanes, J. Geophys. Res., 110, D06109, https://doi.org/10.1029/2004JD005019, 2005.

520